Macromolecules

Article

pubs.acs.org/Macromolecules

How Does a Hyperbranched Chain Pass through a Nanopore?

Lianwei Li,[†] Chen He,[‡] Weidong He,[‡] and Chi Wu*[,†,§]

[†]Hefei National Laboratory for Physical Sciences at Microscale, Department of Chemical Physics, University of Science and Technology of China, Hefei, China 230026

[‡]CAS Key Laboratory of Soft Matter Chemistry, Department of Polymer Science and Engineering, University of Science and Technology of China, Hefei, China 230026

[§]Department of Chemistry, The Chinese University of Hong Kong, Shatin N. T., Hong Kong

ABSTRACT: Starting from seesaw-type linear macromonomer azide∼∼alkyne∼∼azide, where "∼∼" represents polystyrene with a controllable length, we successfully obtained two series of narrowly distributed "defect-free" hyperbranched polystyrenes with an identical subchain length but different overall molar masses or with a similar overall molar mass but different subchain lengths. Our ultrafiltration study reveals that the critical flow rate ($q_{c,b}$) to pull these branched chains through a small cylindrical pore under an elongational flow field depends on both polymerization degrees of the entire chain and the subchain (N_t and N_b) as $q_{c,b} \sim N_t^{\gamma} N_b^{\varphi}$, where γ and φ are 1.0 and −0.4, different from those predicted values $\gamma = 1/3$ and 1/4, and $\varphi = 1/15$ and −1/4 for the weak and strong confinements, respectively. Besides the previously improper assumption of each blob as a hard sphere, such discrepancies are also attributed to (1) a smaller scaling exponent between the size and molar mass of the chain squeezed inside the pore because it is not a chain free in solution and (2) for a given pore size, the hyperbranched chains with different subchain lengths are in different confinements, making the determination of φ less meaningful. In addition, $q_{c,b}$ is related to the pore size (D) as $q_{c,b} \sim D^{-0.8}$. Finally, we have demonstrated that the current quantitative study enables us, *for the first time*, to use small cylindrical pores to separate large hyperbranched chains by their structures (different subchain lengths) and topologies instead of their sizes.

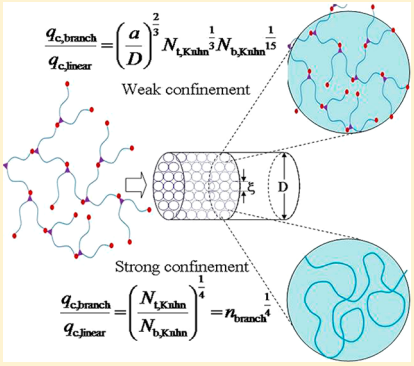

INTRODUCTION

The translocation of flexible polymer chains in solution through a porous media dominates many processes: size exclusion chromatography (SEC),[1] ultrafiltration,[2] and gene delivery,[3] to name but a few. Generally speaking, whether a polymer chain can pass through a pore smaller than its size under an elongational flow should depend on the flow rate and its deformability. The deformability is mainly determined by its chemical and topological structures. Limited by polymer synthesis methodologies, the preparation of "defect-free" star-like or hyperbranched chains is rather difficult, if not impossible, which has hindered experimental confirmation of some predicted behaviors of polymer chains passing through a small pore. Therefore, the application of ultrafiltration in separating polymer chains with a similar hydrodynamic size but different topologies still remains an important challenge in modern polymer research. de Gennes[4] and Pincus[5] predicted that the critical flow rate ($q_{c,linear}$) for a linear chain to pass through a small cylindrical pore with a diameter of D is $q_{c,linear} \sim k_B T/\eta$, where k_B, T, and η are the Boltzmann constant, the absolute temperature, and viscosity, respectively. Our previous study on linear polymer chains passing through the pore confirmed that $q_{c,linear}$ is indeed independent of the chain length but unexpectedly decreases as D increases.[2,6] Using a scaling argument, we showed

$$q_{c,linear} = \frac{k_B T}{3\pi\eta}\frac{D}{l_e} \quad (1)$$

where l_e is the effective length of each "blob" along the flow directio, and l_e is scaled to D as $D = kl_e^{\alpha}$ with k, a solution-dependent constant and $1/2 \le \alpha \le 3/5$, varying with the solvent quality.[7] Here the "blob" is defined as a portion of the confined chain whose center of gravity moves randomly under the thermal agitation. Such a scaling argument was recently supported by the first principles calculation.[8,9] Later, we extended our studies to the ultrafiltration behavior of regular star-like polystyrene chains with different arm lengths (L_A) and arm numbers (f) and found that for a given L_A the critical flow rate of star chains ($q_{c,star}$) dramatically increases with f but is nearly independent of L_A for a given f, contradictory to the de Gennes' prediction[10] because he assumed that each pulled-in arm was fully stretched. Our results reveal that such an assumption is not necessary so that $q_{c,s}$ is simply related to the number of forwarded arms inside the pore (f_{in}),[11,12] i.e.

$$\frac{q_{c,star}}{q_{c,linear}} = \frac{f + |f - 2f_{in}|}{2} \quad (2)$$

It shows that $q_{c,star}$ reaches its minimum at $f_{in} = f/2$, which has been experimentally confirmed, especially when $f \gg 1$. After understanding how a star-like chain passes through a small pore

Received: July 16, 2012
Revised: August 31, 2012
Published: September 14, 2012

   dx.doi.org/10.1021/ma301468z | *Macromolecules* 2012, 45, 7583−7589

Scheme 1. Schematic of How a Number of Seesaw-Type Linear Polystyrene (PS) Macromonomers Are "Clicked" Together To Form a Hyperbranched PS Chain

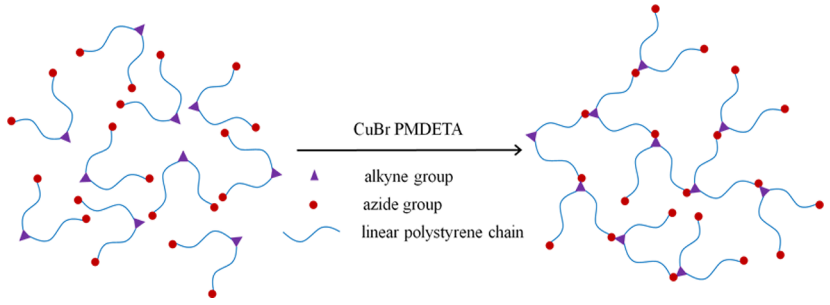

and knowing that $q_{c,star} > q_{c,linear}$, we recently successfully separated a mixture of linear and star-like chains by choosing a flow rate between $q_{c,star}$ and $q_{c,linear}$, realizing a long-time dream of using ultrafiltration to separate polymer chains by their topologies instead of their sizes.[13]

In comparison with linear and star chains, the ultrafiltration of hyperbranched chains is much more complicated because a hyperbranched chain can be weakly or strongly confined inside a pore, depending on both the blob size (ξ) and the subchain length (l_s). Namely, when $\xi \ll l_s$ (sparsely branched polymers with long subchains), each subchain contains a number of blobs, or say, each blob contains a linear chain segment, so that the hyperbranched chain is strongly confined inside the pore; while $\xi \gg l_s$ (densely branched polymers with short subchains), the confinement is weak (the chain does not deform much and each blob contains a number of subchains, or say, a hyperbranched segment). In 1996, using the simple scaling argument, de Gennes et al.[14] deduced the critical flow rate ($q_{c,branch}$) for hyperbranched chains in good solvents and showed that $q_{c,branch}$ depends on both polymerization degrees of the entire chain and the subchain (N_t and N_b); i.e., $q_{c,branch} \sim N_t^{\gamma} N_b^{\varphi}$, where $\gamma = 1/2$ and $2/3$, and $\varphi = -1/2$ and $2/15$ for the strong and weak confinements inside the pore, respectively.

However, such predictions have never been seriously tested by real experiments partially because it is rather difficult to prepare "defect-free" hyperbranched chains with uniform and long subchains between two neighboring branching points as well as in controlling the overall and subchain molar masses. Recently, after designing, preparing and using seesaw-type linear macromonomer B∼∼A∼∼B, where ∼∼, B, and A denote a polystyrene (PSt) chain, azide group, and alkyne group, respectively, we have successfully prepared "defect-free" hyperbranched polystyrenes with uniform subchains defined by the initial length between A and B.[15,16] Our B∼∼A∼∼B strategy is different from those commonly used approaches: A∼∼B_2[17−19] and A∼∼A + B_3[20,21] because they normally lead to a broadly distributed subchains with different lengths because of some unavoidably unreacted B-groups. In our method, azide can only react with alkyne via the click chemistry so that the subchain lengths have a uniform length.

Using two sets of hyperbranched polystyrenes with different overall molar masses but a uniform subchain length or with different subchain lengths but a similar overall molar mass, we first established the scaling laws between their sizes and the overall molar mass as well as the subchain length and then experimentally studied how they are pulled through a pore by using a previously established ultrafiltration method; namely, we have experimentally scaled $q_{c,branch}$ to both N_t and N_b and explained discrepancies between our results and those predicated values. Finally, using two hyperbranched polystyrenes with a similar size but different subchain lengths, we showed how one can use such established quantitative scaling laws to separate hyperbranched chains by their structure and topology instead of their size.

EXPERIMENTAL SECTION

Sample Preparation. Scheme 1 schematically shows how seesaw-type linear macromonomer azide∼∼alkyne∼∼azide chains are "clicked" together to form a hyperbranched polystyrene chain. The synthesis procedure was detailed before.[16] Such prepared hyperbranched polymer chains are normally broadly distributed in their overall molar masses. We further fractionated each resultant hyperbranched sample in a toluene/methanol mixture into a series of narrowly distributed chains with different overall molar masses characterized by laser light scattering.

The fractionation was done as follows: (1) the sample was dissolved in toluene at room temperature with a concentration around 0.01 g/mL in a round-bottom flask, (2) methanol was slowly dropped in until the solution became milky, (3) the solution temperature controlled by a water bath (±0.1 °C) was slightly raised until the solution became clear again, (4) the solution was slowly cooled down until it became slightly milky, and (5) the solution temperature was maintained to allow a very small fraction of longest chains to precipitate. Repeating steps 2−5 led to fractions with different overall molar masses. The characterization of macromonomers used in our experiments is summarized in Table 1.

Table 1. Size Exclusion Chromatography Characterization of Linear Polystyrene Macromonomers Prepared by ARGET ATRP

macromonomer	M_n (g/mol)	M_w (g/mol)	M_w/M_n
PSt-73K	6.30×10^4	7.30×10^4	1.15
PSt-21K	1.90×10^4	2.10×10^4	1.11
PSt-8.8K	8.10×10^3	8.80×10^3	1.09

It shows that initial macromonomer linear chains are narrowly distributed, ensuring that the length of subchains between two neighboring branching points is uniform for each hyperbranched polystyrene sample.

Laser Light Scattering. A commercial LLS spectrometer (ALV/DLS/SLS-5022F) equipped with a multi-τ digital time correlator (ALV5000) and a cylindrical 22 mW Uniphase He−Ne laser (λ_0 = 632.8 nm) as the light source was used. In static LLS,[22,23] the angular dependence of the absolute excess time-average scattering intensity, known as the Rayleigh ratio $R_{VV}(q)$, can lead to the weight-average molar mass (M_w), the root-mean-square gyration radius $\langle R_g^2 \rangle_z^{1/2}$ (or simply written as $\langle R_g \rangle$), and the second virial coefficient A_2 by using

$$\frac{KC}{R_{VV}(q)} \cong \frac{1}{M_w}\left(1 + \frac{1}{3}\langle R_g^2 \rangle_z q^2\right) + 2A_2C \qquad (3)$$

where $K = 4\pi^2(dn/dC)^2/(N_A\lambda_0^4)$ and $q = (4\pi/\lambda_0)\sin(\theta/2)$ with C, dn/dC, N_A, and λ_0 being the concentration of the polymer solution,

dx.doi.org/10.1021/ma301468z | Macromolecules 2012, 45, 7583−7589

the specific refractive index increment, Avogadro's number, and the wavelength of light in a vacuum, respectively. The extrapolation of $R_{VV}(q)$ to $q \to 0$ and $C \to 0$ leads to M_w. The plot of $[KC/R_{VV}(q)]_{C\to 0}$ vs q^2 and $[KC/R_{VV}(q)]_{q\to 0}$ vs C lead to $\langle R_g^2\rangle_z$ and A_2, respectively. In a very dilute solution, the term of $2A_2C$ can be ignored. For relatively small scattering objects, the Zimm plot on the basis of eq 3 incorporates the extrapolations of $q \to 0$ and $C \to 0$ on a single grid. For large hyperbranched chains, i.e., $q\langle R_g\rangle > 1$, the Berry plot is normally used. The scattering intensity at each angle was recorded 30 s × 3 times and averaged. The scattering angle ranges from 12° to 120°. The refractive index increment of hyperbranched polystyrenes in toluene (dn/dC = 0.111 mL/g at 25 °C and 633 nm) was determined by a highly accurate differential refractometer.[24]

In dynamic LLS,[25] the Laplace inversion of each measured intensity−intensity time correlation function $G^{(2)}(q,t)$ in the self-beating mode can lead to a line-width distribution $G(\Gamma)$, where q is the scattering vector. For dilute solutions, Γ is related to the translational diffusion coefficient D by $(\Gamma/q^2)_{q\to 0,C\to 0} \to D$, so that $G(\Gamma)$ can be converted into a transitional diffusion coefficient distribution $G(D)$ or further a hydrodynamic radius distribution $f(R_h)$ via the Stokes−Einstein equation, $R_h = (k_BT/6\pi\eta_0)/D$, where k_B, T, and η_0 are the Boltzmann constant, the absolute temperature, and the solvent viscosity, respectively. The polydispersity index M_w/M_n was estimated from $M_w/M_n \approx (1 + 4\,\mu_2/\langle D\rangle^2)$, where $\mu_2 = \int_0^\infty G(D)(D - \langle D\rangle)^2\,dD$. In dynamic LLS experiments, we used a fixed small angle (12°) to ensure that the correction of extrapolating the scattering angle to zero is less important. The time correlation functions were analyzed by both the cumulants and CONTIN analysis.

Ultrafiltration. In our current ultrafiltration experiments, commercially available anodic aluminum oxide double layer membranes (Whatman, Anotop 10) were used. The thicknesses (pore diameters) of the top and bottom layers are 59 μm (200 nm) and 1 μm (20 or 100 nm), respectively. The two layers contain a nearly equal number of cylindrical pores; namely, each smaller pore is under a large 200 nm one, which prevents possible interference of the flow fields generated by different small pores at their entrances; i.e., each smaller pore is isolated, so that our study nearly resembles a single pore experiment even many pores are actually used. In each solution, we added an appropriate amount of short linear polystyrene chains with a size smaller than the small pore. They can pass through the small pore by diffusion even without any flow so they served as an internal standard. The concentrations of large hyperbranched chains and short linear chains (C_L and C_S) are properly chosen so that $\langle I_L\rangle/\langle I_S\rangle = C_LM_L/C_SM_S \sim 1.5$, where M_L and M_S are the molar masses of hyperbranched and short linear chains, respectively. Note that in dynamic LLS $\langle I_L\rangle/\langle I_S\rangle$ equals the area ratio of their corresponding peaks in $G(\Gamma)$. Since there is no retention for the short linear chains, a decrease of $\langle I_L\rangle/\langle I_S\rangle$ is related to the retention of large hyperbranched chains, enabling us to calculate their relative retention $[(C_0 - C)/C_0]$ under each flow rate, where C_0 and C are polymer concentrations before and after the ultrafiltration.[2] The solution temperature and flow rate were controlled by an incubator (Stuart Scientific, S160D) (±0.2 °C) and a syringe pump (Harvard Apparatus, PHD 2000), respectively.

RESULTS AND DISCUSSION

Our previous studies showed that both the average radius of gyration ($\langle R_g\rangle$) and the average hydrodynamic radius ($\langle R_h\rangle$) of hyperbranched chains are scaled to both the polymerization degrees of the entire chain (N_t) and the subchain (N_b). In theory,[26−28] $\langle R\rangle \sim N_t^{\alpha}N_b^{\beta}$ with $\alpha = 1/2$ and $\beta = 1/10$. Our measured $\alpha = 0.46 \pm 0.01$ for $\langle R_g\rangle$ and $\alpha = 0.48 \pm 0.01$ for $\langle R_h\rangle$, smaller than the predicted 1/2, and $\beta = 0.11 \pm 0.01$ for $\langle R_g\rangle$ and 0.09 ± 0.01 for $\langle R_h\rangle$, close to the predicted 1/10. The smaller measured values of α are expected because the hydrodynamic interaction and excluded volume are not considered in previous theories.

Armed with these narrowly distributed "defect-free" hyperbranched chains, we were able to start the ultrafiltration experiments by gradually changing the flow rate and measuring the relative retention $[(C_0 - C)/C_0]$. Figure 1 shows that $(C_0 - C)/C_0$

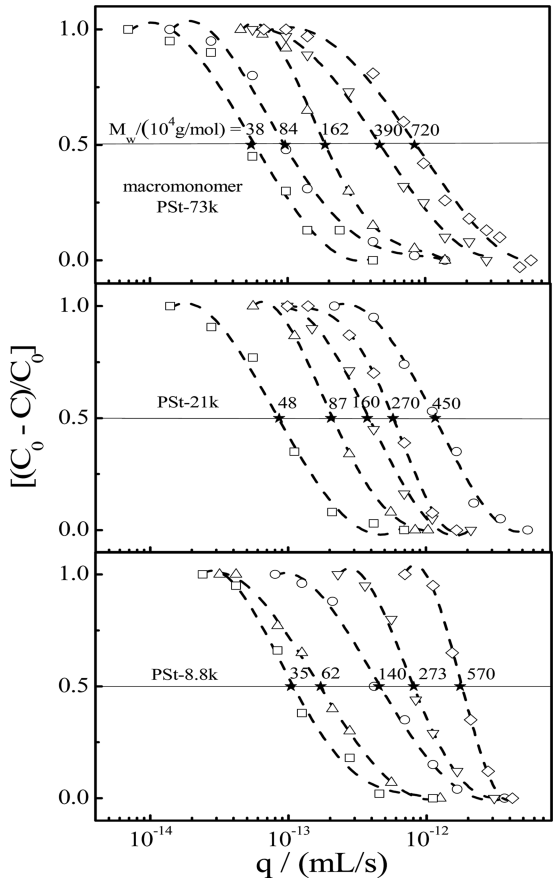

Figure 1. Flow rate (q) dependence of relative retention $[(C_0 - C)/C_0]$ of hyperbranched polystyrene chains made of different macromonomers in toluene at T = 25 °C, where the symbol "*" marks $q_{c,b,50\%}$.

decreases as the flow rate increases but not as sharp as the first-order coil-to-stretch transition of linear chains observed before.[2] Presumably, this is because even for a given overall molar mass (M_w), different arrangements of a given number of uniform subchains can lead to different hyperbranched chain structures. As expected, the flow rate required to pull the hyperbranched chains to pass through the pore increases with N_t for each given N_b.

Figure 2 shows that the critical flow rate ($q_{c,b,50\%}$) of the hyperbranched chains with a given subchain length is scaled to the polymerization degree of entire hyperbranched chain (N_t) as $q_{c,b,50\%} \sim N_t^{\gamma}$ with $\gamma = 1.0 \pm 0.1$. We also differentiated each curve in Figure 1 and plotted $q_{c,b,peak}$, $q_{c,b,20\%}$, or $q_{c,b,80\%}$ against N_t. The scaling exponent (γ) remains 1.0 ± 0.1. For a given N_t, $q_{c,b,50\%}$ decreases as the subchain length increases because longer subchains deform easier inside the pore so that a low flow rate is required to pull each hyperbranched chain through. Further, we fixed N_t to find how $q_{c,b,50\%}$ is scaled to N_b. Our results showed that $\varphi = -0.4 \pm 0.1$ with a large uncertainty because there are only three data points within a limited range of N_b. Even considering our experimental uncertainties, our measured scaling laws are still deviated much from $q_{c,b} \sim N_t^{1/3}N_b^{1/15}$ and $q_{c,b} \sim N_t^{1/4}N_b^{-1/4}$, respectively, predicted for the weak and strong confinements,[12] which forces us to reconsider whether something was missing or improper in the original

dx.doi.org/10.1021/ma301468z | Macromolecules 2012, 45, 7583−7589

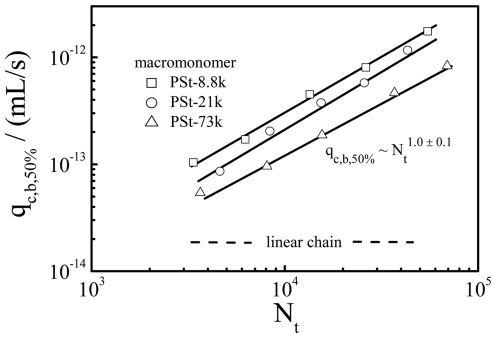

Figure 2. Overall polymerization degree (N_t) dependence of critical flow rate ($q_{c,b,50\%}$) of hyperbranched chains made of different seesaw-type macromonomers (i.e., subchain lengths) in toluene at T = 25 °C.

assumption and theoretical treatments of how hyperbranched chains pass through a small cylindrical pore under an elongation flow. It is worth noting that such theoretical predictions have never been experimentally tested or confirmed before.

As discussed before, each hyperbranched chain confined inside a small cylindrical pore can be viewed as a number of packed "blobs", and each blob has a size (correlation length) of ξ and contains n number of Kuhn segments, as schematically shown in Scheme 2. In the limit of the weak or strong confinements,

Scheme 2. Schematic of Weak and Strong Confinements of a Hyperbranched Chain inside a Small Cylindrical Pore with a Diameter of D, Where Each Small Circle Represents a Blob with a Size of ξ

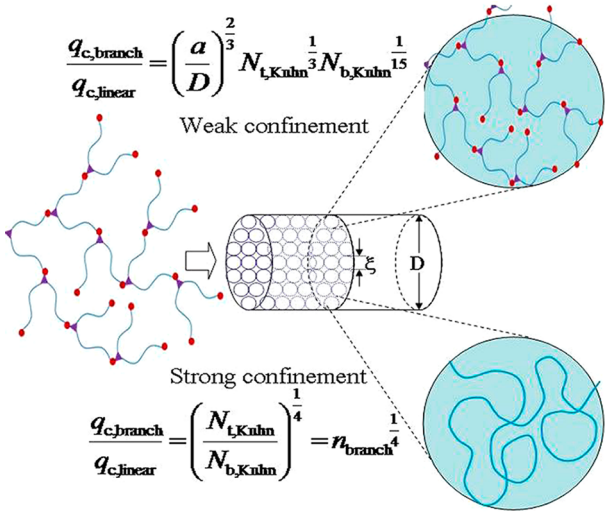

each blob contains a hyperbranched or a linear chain segment, i.e., $\xi = aN_{t,Kuhn}^{1/2}N_{b,Kuhn}^{1/10}$ or $aN_{t,Kuhn}^{3/5}$ in good solvents, where a is the size of a Kuhn monomer and $N_{t,Kuhn}$ and $N_{b,Kuhn}$ are numbers of the Kuhn segments of the entire hyperbranched chain and the subchain, respectively. Obviously, the maximum size of a blob is the pore diameter (D); namely, $\xi \leq D$. Previously, we showed that instead of considering the entire confined chain, one only needs to balance the confinement and hydrodynamic forces on each blob and found a unified description of q_c for chains with different topologies, i.e.[12]

$$\frac{q_c}{q_{c,linear}} = \left(\frac{D}{\xi}\right)^2 \tag{4}$$

which is different from what de Gennes previously derived,[10] wherein $q_{c,branch}/q_{c,linear} = (D/\xi)^4$ (eq 30 in ref 10) was incorrect because the barrier energy (E_b) of one layer of the blobs was mistaken as $\sim k_BT$. Actually, k_BT is the barrier energy for one blob. The barrier energy for one layer of the blobs in the cross section of the pore should be k_BT multiplied by the number of the blobs in one layer, i.e., $E_b = k_BT(D^2/\xi^2)$. This is why the exponent changes from 4 to 2 in eq 4.

Here the only thing left is to find ξ for each chain topology. Obviously, for a confined linear chain, $\xi = D$; while for a confined star chain with a total of f arms and a number of forwarded arms inside the pore (f_{in}), we showed how $q_{c,star}$ depends on f and f_{in} in the Introduction. As for hyperbranched chains, we previously derived[12]

$$\frac{q_{c,branch}}{q_{c,linear}} = \left(\frac{a}{D}\right)^{2(3-5\alpha)/[3(3\alpha-1)]} N_{t,Kuhn}{}^{\gamma} N_{b,Kuhn}{}^{\phi} \tag{5}$$

with

$$\gamma = \frac{\alpha}{3(3\alpha-1)} \text{ and } \phi = \frac{6\beta-\alpha}{3(3\alpha-1)}$$

where α and β are two scaling constants defined before, i.e., $\langle R_g^2\rangle^{1/2} = aN_{t,Kuhn}{}^{\alpha}N_{\beta,Kuhn}{}^{\beta}$, which is well-documented in the literature and books.[7,26−28] It is worth noting that eq 5 covers different solvent qualities and chain confinements. For the weak confinement, as shown in Scheme 2, each blob contains a small hyperbranched chain segment so that $\alpha = 1/2$ and $\beta = 1/10$ in good solvents. In this case, eq 5 can be rewritten as

$$\frac{q_{c,branch}}{q_{c,linear}} = \left(\frac{a}{D}\right)^{2/3} N_{t,Kuhn}{}^{1/3} N_{b,Kuhn}{}^{1/15} = \left(\frac{a}{D}\right)^{2/3} n_{branch}{}^{1/3} N_{b,Kuhn}{}^{6/15} \quad \text{(weak confinement)} \tag{6a}$$

where n_{branch} is the number of branching points inside a hyperbranched chain and defined as $N_{t,Kuhn}/N_{b,Kuhn}$. While for the strong confinement, each blob contains a linear chain segment, as schematically shown in Scheme 2. Therefore, $\alpha = 3/5$ and $\beta = 0$ so that we have

$$\frac{q_{c,branch}}{q_{c,linear}} = \left(\frac{N_{t,Kuhn}}{N_{b,Kuhn}}\right)^{1/4} = n_{branch}{}^{1/4} \quad \text{(strong confinement)} \tag{6b}$$

For linear chains, $N_{t,Kuhn} = N_{b,Kuhn}$, i.e., $n_{branch} = 1$ so that $q_{c,branch} = q_{c,linear}$, as expected. The crossover between these two confinement limits occurs when D approaches a critical value (D^*) at which the subchain and the pore have a similar size. Quantitatively, we can calculate it by equaling the right-hand sides of eqs 6a and 6b, namely

$$D^* = aN_{t,Kuhn}{}^{1/8}N_{b,Kuhn}{}^{19/40} \tag{7}$$

It shows that D^* weakly depends on the overall molar mass but more on the subchain length. For polystyrene in toluene, it is known that each Kuhn segment contains ~7 monomers and has a size of ~1.8 nm.[29] If ξ reaches D (its maximum value, 20 nm), each blob only contains ~55 and ~100 Kuhn segments in the strong and weak confinements, respectively. For the three hyperbranched polystyrenes used here, their subchains respectively contain ~5, ~15, and ~50 Kuhn segments. Therefore, even for the hyperbranched polystyrene made of

dx.doi.org/10.1021/ma301468z | Macromolecules 2012, 45, 7583−7589

the shortest subchain, each blob mostly contains ~20 subchains, i.e., ~10 branching points. In reality, ξ is much smaller than D so that each blob contains few branch points. In other words, the chain topology inside each blob is not ideally branched but star-like. As for the hyperbranched polystyren sample made of the longest subchain, each subchain might contain few blobs.

Quantitatively, letting D^* to be the pore size (20 nm), we are able to estimate the boundary that divides the two confinements, as shown in Figure 3. It is clear that for the hyperbranched

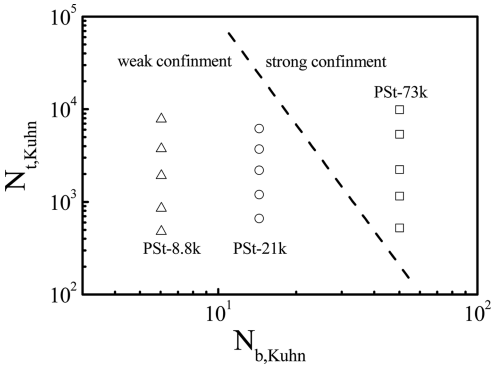

Figure 3. Calculated "phase" diagram of strong and weak confinements of hyperbranched polystyrene chains in toluene at T = 25 °C, where dashed line represents a boundary between two different confinements, where we used D^* = 20 nm, a ± 1.8 nm, and $N_{b,Kuhn}$ ± $7N_b$ (ref 29).

polystyrene chains made of the two short macromonomers (PSt-8.8K and PSt-21K) the ultrafiltration occurs in the weak confinement region, while the hyperbranched polystyrenes made of the longest macromonomer (PSt-73K) are on the strong confinement side, but far away from the weak or strong confinement limit, because the pore and subchain have a similar size. In other words, most of our ultrafiltration experiments were done around the weak and strong confinement boundary. Therefore, we are not able to use eq 6 to treat our experimental data, which also partially explains why the scaling exponents are deviated from the predicted ones.

On the basis of eqs 5 and 6, we know that γ increases from 1/4 to 1/3 when α decreases from 3/5 to 1/2, as shown in Figure 4. Putting our experimentally measured α = 0.46 ± 0.01

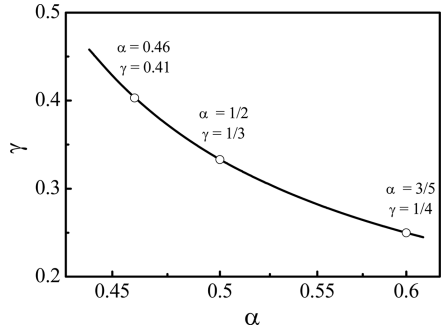

Figure 4. Plot of two scaling exponents α versus γ based on eq 6.

into eq 5, we have γ = 0.41, still far away from 1.0 ± 0.1, as shown in Figure 3, even after considering all the experimental uncertainties. Physically, for a given overall molar mass, a smaller α means a more compact and less deformable chain conformation so that a higher flow rate is required to drag the chain into the pore, resulting in a stronger molar-mass-dependent critical flow rate. Therefore, the higher measured γ value actually means that the real α value should be smaller. Putting the measured γ value into eq 6, we are able to estimate that α ± 3/8, which is reasonable because the chain segments inside each blob are squeezed together with a more uniform chain density so that α should be lower than that for the hyperbranched chain free in solutions. In the fully collapsed limit, α = 1/3 for a subject with a uniform density. It is worth noting that such a discrepancy might also be traced back to the assumption of the blob as a nondraining sphere.

On the other hand, φ depends on both α and β. As α decreases from 3/5 to 1/2 and β increases from 0 to 1/10, φ increases from −1/4 to 1/15. Equation 6 generally shows that a smaller α should lead to a larger φ. In the current study, the chain topology inside the blob changes from branching to star-like and then to linear as the subchain length increases. Therefore, it is not meaningful to extract φ from our current study. In reality, using shorter initial subchains in the polymerization results in smaller hyperbranched chains, while using much longer initial subchains leads to a low reactivity, which limit the reachable ranges of $N_{t,Kuhn}$ and $N_{b,Kuhn}$.

Figure 5 further shows how the pore size (D) affect $q_{c,branch}$. The slope of $q_{c,branch}$ versus D is slightly smaller than −2/3

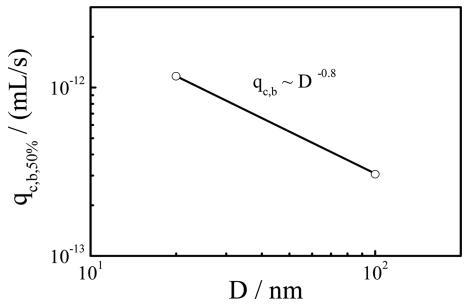

Figure 5. Pore size (D) dependence of critical flow rate ($q_{c,branch,50\%}$) of fraction made of macromonomer PSt-21K with N_t = 4.33 × 10^4.

predicted by eqs 5 and 6. Since there are only two points, we *could not* and *should not* be too serious about the value of the slope. Besides the experimental uncertainties, such a deviation can be similarly explained as what we did for linear chains.[6,8,9] Namely, each blob contains a chain segment, not a hard sphere, so that it is draining. Therefore, the effective length of each blob (l_e) along the flow direction is longer than its size (ξ) and l_e is proportional to the molar mass of the chain segment inside the blob and scaled to ξ with a scaling exponent that depends on the topology of the chain segment inside the blob.

Up to now, we have discussed how the molar masses of the overall chain and the subchain affect the ultrafiltration of a hyperbranched chain through a small cylindrical pore. Note that our ultimate goal of conducting this kind of studies is to use what we found/understood to separate polymer chains by their structures, such as the subchain length and the overall molar mass, instead of those existing methods mainly by the hydrodynamic volume and solubility. Using the following example, we like to demonstrate how it works in a real application to effectively separate hyperbranched chains with a similar size but different subchain lengths.

As shown in eqs 5 and 6, for a given overall molar mass ($N_{t,Kuhn}$), hyperbranched chains with a shorter subchain (i.e., a higher branching density) require a higher critical flow rate to

dx.doi.org/10.1021/ma301468z | Macromolecules 2012, 45, 7583−7589

pull them through a given cylindrical pore due to its weaker deformability, which leads us to separate hyperbranched polymer chains with a similar overall molar mass or hydrodynamic volume, but different branching degrees by flushing a mixture of them through small pores with a properly chosen flow rate. To demonstrate it, we purposely chose two hyperbranched samples, and their molecular parameters (the weight-average molar mass (M_w), polydispersity index (M_w/M_n), and average hydrodynamic radius ($\langle R_h \rangle$)) are summarized in Table 2, where

Table 2. Molecular Parameters of Two Hyperbranched and One Short Linear Chains

polymer	$M_{w,macromonomer}$ (kg/mol)	M_w (kg/mol)	M_w/M_n	$\langle R_h \rangle$ (nm)
HB-3.3K	3.3	780	1.13	21
HB-73K	73	840	1.10	27
linear PS as an internal reference		11	1.05	2.6

a linear polystyrene sample was used as an internal reference to calibrate the concentrations of hyperbranched chains before and after the ultrafiltration.

Figure 6A shows that when the flow rate is 4.0×10^{-11} mL/s, much higher than $q_{c,HB\text{-}3.3K}$ and $q_{c,HB\text{-}73K}$, both of the two

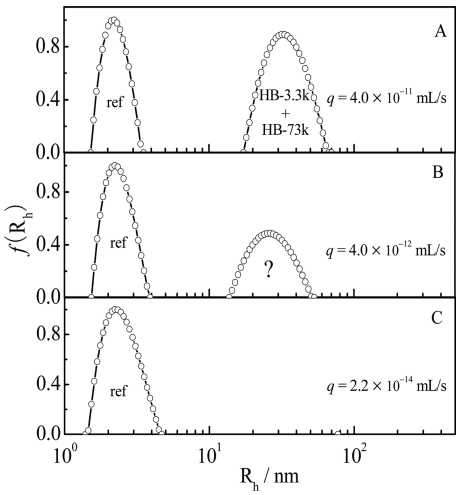

Figure 6. Hydrodynamic radius distribution of a solution mixture of linear reference and two hyperbranched chains (HB-3.3K and HB-73K) in toluene at T = 25 °C after they are extruded through small cylindrical pores (20 nm) under different flow rates, where C_{ref} = 40 mg/mL, $C_{HB\text{-}3.3K}$ = 0.6 mg/mL, and $C_{HB\text{-}73K}$ = 0.5 mg/mL.

hyperbranched chains are able to pass through small pores because we know the ratio of the peak areas between the two hyperbranched and short linear reference chains. As the flow rate decreases to 4.0×10^{-12} mL/s, higher than $q_{c,HB\text{-}73K}$ (1.0×10^{-13} mL/s) but still much lower than $q_{c,HB\text{-}3.3K}$, we also observed two peaks, as shown in Figure 6B, in which the area of the peak located at ~25 nm decreases by ~50% and its position shifted to the left by ~4 nm. In comparison with the solution mixture before the ultrafiltration and data in Table 2, we know, in principle, that here smaller HB-3.3K chains with a short subchain length and a higher branching degree are retained by small cylindrical pores because it is relatively difficult to deform a hyperbranched chain with a shorter subchain (a higher branching degree) when two hyperbranched chains have a similar overall molar mass. As expected, Figure 6C shows that further decrease of the flow rate to 2.2×10^{-14} mL/s makes the peak on the right disappearing because both of the hyperbranched chains are retained by small pores.

For an attentive reader, there still remains a question whether the peak on the right in Figure 6B is truly related to smaller hyperbranched HB-3.3K, instead of larger HB-73K chains that pass though small cylindrical pores. To clarify this point, we mixed the linear reference chains with HB-3.3K and HB-73K, respectively, to prepare two solution mixtures. As shown in Figure 7A, larger hyperbranched HB-73K chains pass through

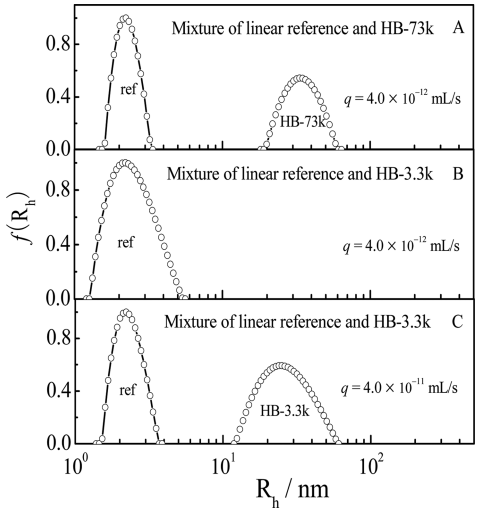

Figure 7. Hydrodynamic radius distributions of mixtures of linear reference with hyperbranched HB-3.3K and HB-73K chains in toluene at T = 25 °C after they are extruded through small cylindrical pores (20 nm) under different flow rates, where C_{ref} = 40 mg/mL, $C_{HB\text{-}73K}$ = 0.6 mg/mL, and $C_{HB\text{-}3.3K}$ = 0.8 mg/mL.

when the flow rate reaches 4.0×10^{-12} mL/s, while smaller hyperbranched HB-3.3K chains are still retained; i.e., its related peak is missing in Figure 7B in comparison with Figure 7C. It requires a flow rate 10 times higher to push smaller hyperbranched HB-3.3K chains to pass through small cylindrical pores (Figure 7C), clearly answering the question. It experimentally demonstrates that one can use small pores to separate hyperbranched chains by their structures instead of their sizes.

Please note that the method and principle demonstrated in this and previous related studies are readily applicable in real situation. Namely, coupling an ultrafiltration system (a filter with a proper pore size and a syringe pump) with an one-angle (90°) dynamic LLS instrument with a stoppable flow cell or a GPC will lead to a workable device in research laboratories to separate and characterize polymer chains with different topologies by using critical flow rates quantitatively established for different chains. We are currently working in developing such a device by integrating our ultrafiltration system into a portable three-angle particle sizing instrument based on dynamic LLS principle. The same principle also applies to real industrial applications. There already exist many different ultrafiltration systems. How to prepare large filters with small cylindrical pores and sufficient mechanic strength will be a real challenge.

■ CONCLUSION

"Defect-free" hyperbranched polystyrenes with uniform and long subchains can be prepared from seesaw-type linear macromonomers,

dx.doi.org/10.1021/ma301468z | Macromolecules 2012, 45, 7583−7589

azide∼∼alkyne∼∼azide, where ∼∼ represents a polystyrene chain. Our ultrafiltration experiments have, *for the first time*, revealed that the critical flow rate ($q_{c,b}$) for hyperbranched chains is indeed dependent on both N_t and N_b; namely, $q_{c,branch} \sim N_t^{1.0\pm0.1} N_b^{-0.4\pm0.1}$. These two exponents deviate from previously predicted ones, which can be attributed to three possible reasons as follows: (1) the chain segment inside each blob is squeezed with a more uniform chain density so that it has a lower scaling exponent (α = 3/8 instead of 1/2); (2) the chain segment inside each blob is not a hard sphere but draining; and (3) the topology of the chain segment inside each blob changes when we use the hyperbranched polystyrenes with different subchain lengths in the current study. Further, we confirmed that $q_{c,branch}$ decreases as D increases, i.e., $q_{c,b} \sim D^{-0.8}$, where the exponent is close to the predicted −2/3. Experimentally, we have, *for the first time*, demonstrated that using the ultrafiltration of hyperbranched polymer chains through small cylindrical pores, we can effectively separate them by their structures instead of their sizes. In comparison with linear and star-like chains, a much higher flow rate is required to pull a hyperbranched chain with a similar size though a cylindrical pore. After quantitatively understanding how polymer chains with different topologies pass though a small cylindrical pore, we are now able to use a properly chosen flow rate to separate them by their topologies instead of their sizes.

AUTHOR INFORMATION

Corresponding Author

*The Hong Kong address should be used for correspondence. E-mail: chiwu@cuhk.edu.hk.

Notes

The authors declare no competing financial interest.

ACKNOWLEDGMENTS

The financial support of the National Natural Scientific Foundation of China Projects (20934005 and 51173177), the Ministry of Science and Technology of China (Key Project, 2012CB933802), and the Hong Kong Special Administration Region Earmarked Projects (CUHK4042/10P, 2130241, CUHK4036/11P, 2130281) is gratefully acknowledged.

REFERENCES

(1) Wang, Y.; Teraoka, I.; Hansen, F. Y.; Peters, G. H.; Hassager, O. *Macromolecules* **2010**, *44*, 403.
(2) Jin, F.; Wu, C. *Phys. Rev. Lett.* **2006**, *96*, 237801.
(3) Cai, J.; Yue, Y.; Rui, D.; Zhang, Y.; Liu, S.; Wu, C. *Macromolecules* **2011**, *44*, 2050.
(4) de Gennes, P. G. *J. Chem. Phys.* **1974**, *60*, 5030.
(5) Pincus, P. *Macromolecules* **1976**, *9*, 386.
(6) Ge, H.; Jin, F.; Li, J.; Wu, C. *Macromolecules* **2009**, *42*, 4400.
(7) Flory, P. J. *Principles of Polymer Chemistry*; Cornell University Press: Ithaca, NY, 1953.
(8) Freed, K. F.; Wu, C. *J. Chem. Phys.* **2011**, *135*, 144902.
(9) Freed, K. F.; Wu, C. *Macromolecules* **2011**, *43*, 9863.
(10) de Gennes, P. G. *Adv. Polym. Sci.* **1999**, *38*, 92.
(11) Ge, H.; Pispas, S.; Wu, C. *Polym. Chem.* **2011**, *2*, 1071.
(12) Wu, C.; Li, L. *Polym. Chem.* **2012**, submitted for publication.
(13) Ge, H.; Wu, C. *Macromolecules* **2010**, *43*, 8711.
(14) Gay, C.; de Gennes, P. G.; Raphael, E.; Brochard-Wyart, F. *Macromolecules* **1996**, *29*, 8379.
(15) He, C.; Li, L.; He, W.; Jiang, W.; Wu, C. *Macromolecules* **2011**, *44*, 6233.
(16) Li, L.; He, C.; He, W.; Wu, C. *Macromolecules* **2011**, *44*, 8195.
(17) Hutchings, L. R. *Soft Matter* **2008**, *4*, 2150.
(18) Clarke, N.; Luca, E. D.; Dodds, J. M.; Kimani, S. M.; Hutchings, L. R. *Eur. Polym. J.* **2008**, *44*, 665.
(19) Li, J.; Sun, M.; Bo, Z. *J. Polym. Sci., Part A: Polym. Chem.* **2007**, *45*, 1084.
(20) Unal, S.; Yilgor, I.; Yilgor, E.; Sheth, J. P.; Wilkes, G. L.; Long, T. E. *Macromolecules* **2004**, *37*, 7081.
(21) Unal, S.; Ozturk, G.; Sisson, K.; Long, T. E. *J. Polym. Sci., Part A: Polym. Chem.* **2008**, *46*, 6285.
(22) Zimm, B. H. *J. Chem. Phys.* **1948**, *16*, 1099.
(23) Chu, B. *Laser Scattering*, 2nd ed.; Academic Press: New York, 1991.
(24) Wu, C.; Xia, K. *Rev. Sci. Instrum.* **1994**, *65*, 587.
(25) Berne, B.; Pecroa, R. *Dynamic Light Scattering*; Plenum Press: New York, 1976.
(26) Isaacson, J.; Lubensky, T. C. *J. Phys., Lett.* **1980**, *41*, 469.
(27) Render, S. *J. Phys. A: Math. Gen.* **1979**, *12*, L239.
(28) Zimm, B. H.; Stockmayer, W. H. *J. Chem. Phys.* **1949**, *17*, 1301.
(29) Rubinstein, M.; Colby, R. H. *Polymer Physics*; Oxford University Press: New York, 2003.